ARTICLE IN PRESS

Climate Risk Management xxx (2016) xxx–xxx

Contents lists available at ScienceDirect

Climate Risk Management

journal homepage: www.elsevier.com/locate/crm

Regional climate change trends and uncertainty analysis using extreme indices: A case study of Hamilton, Canada

Tara Razavi [a,c,*], Harris Switzman [b,1], Altaf Arain [c], Paulin Coulibaly [a,c]

[a] McMaster University, Department of Civil Engineering, 1280 Main Street West, Hamilton, Ontario L8S 4L7, Canada
[b] Ontario Climate Consortium/Toronto and Region Conservation, Toronto, Ontario, Canada
[c] McMaster University, School of Geography and Earth Sciences, 1280 Main Street West, Hamilton, Ontario L8S 4L7, Canada

ARTICLE INFO

Article history:
Received 17 December 2015
Revised 13 June 2016
Accepted 14 June 2016
Available online xxxx

Keywords:
Climate change
Uncertainty
Trend
Downscaling
Precipitation
Temperature

ABSTRACT

This study aims to provide a deeper understanding of the level of uncertainty associated with the development of extreme weather frequency and intensity indices at the local scale. Several different global climate models, downscaling methods, and emission scenarios were used to develop extreme temperature and precipitation indices at the local scale in the Hamilton region, Ontario, Canada. Uncertainty associated with historical and future trends in extreme indices and future climate projections were also analyzed using daily precipitation and temperature time series and their extreme indices, calculated from gridded daily observed climate data along with and projections from dynamically downscaled datasets of CanRCM4 and PRECIS, and the statistically downscaled CIMP5 ensemble. A bias correction technique was applied to all raw daily temperature and precipitation time series prior to calculation of the indices.

All climate models predicted increasing trends for extreme temperature indices, maximum 1-day and 5-day precipitation (RX1day and RX5day), total wet day precipitation (PRCPTOT), very heavy precipitation days (R20mm), Summer Days (SU), and Tropical Nights (TR) and decreasing trend for Forest Days (FD) and Ice Days (ID) in 2020s, 2050s, and 2080s compared to present. CanRCM4 model did consistently project values in the upper range of the CMIP5 ensemble while the PRECIS ensemble was more in-line with the CMIP5 mean values. This difference may however be a function of different emission scenarios used.

1. Introduction

Characterizations of historical and future trends in climate, along with their uncertainty are frequently used at the local-scale to understand of how climate change influences the frequency and intensity of extreme weather. This information is regarded as critical to assessing and developing strategies for managing and mitigating the impacts of climate change on local communities (IPCC, 2012). Many climate change impact assessment and risk management tools recommend that decision makers employ some form of quantitative downscaled climate projection in order to characterize changes in the frequency and intensity of extreme weather events for various future time horizons relevant to the business areas in

* Corresponding author.
E-mail address: razaviz@mcmaster.ca (T. Razavi).
[1] Currently with WaterSMART Solutions Ltd.

http://dx.doi.org/10.1016/j.crm.2016.06.002
2212-0963/

question (Engineers Canada, 2015; Field et al., 2014; ICLEI, 2010; IPCC, 2012; PNW Tribal Climate Change Project, 2013; Swanston and Janowiak, 2012). These estimates can be used in "top-down" or "bottom-up" climate change assessment and response frameworks (Bhave et al., 2014; Brown and Wilby, 2012; Brown et al., 2012; Wilby et al., 2014) and relied upon heavily in the development of the "probability" or "likelihood" within a typical risk score used in adaptation decision making (e.g., Engineers Canada PIEVC). The characterization of trends and uncertainty in climate extremes is also useful in the derivation of time series for input to process models used in wide array of planning and management sectors, such as the hydrologic models used in flood risk management (e.g., Seidou et al., 2012; Wilby and Keenan, 2012), ecological impact models (e.g., Baró et al., 2014; Candau and Fleming, 2011; Matthews et al., 2014), water allocation and source protection (EBNFLO Environmental and AquaResource Inc., 2010; Pasini et al., 2012; Zhou et al., 2010), and crop yield models (e.g., Kang et al., 2009), to name a few. As such, having a sense of how strongly we may detect these trends despite uncertainty associated with climate model outputs is critical for developing reliable decision support tools.

Despite the importance of having information on future climate trends, there is no definitive guidance, for Canadian jurisdictions in particular, on which datasets, downscaling methods and extreme indices may be used. Charron (2014) provides some guidance on the types of datasets available, but individual users are still faced with the challenge of selecting the specific datasets and indices to use in their planning processes. Extreme indices also tend to exhibit greater uncertainty than averages (Yao et al., 2013), and this adds an additional challenge to the development of information for use in climate change assessment and planning.

The ensemble approach to climate model analysis is widely recognized as being a reliable and efficient way of elucidating local trends associated with climate change while also characterizing uncertainties associated with projecting future climate, particularly for use in hydrologic modeling (Honti et al., 2014; Velázquez et al., 2012). There are however, many possible ways of constructing an ensemble of future climates that captures the full range of uncertainty associated with greenhouse gas emission scenarios, global circulation model (GCM), and downscaling methods. Each of these potential elements within an ensemble (e.g., emission scenario, GCM, and downscaling) greatly influences the outcome of an individual time series, which might also vary by location and time horizon of interest. To effectively assess future climate trends in light of this uncertainty, it is often advised that users construct and analyse an ensemble that incorporates data from a range of GCMs, downscaling methods, and emission scenarios (EBNFLO and AquaResource, 2010; IPCC, 2014).

Utilization of ensemble or multi-model datasets for future climate projections has the advantage of capturing full range of possible climate change scenarios. It also has the advantage of accounting for minimizing the effect of possible biases associated with individual models and can therefore provide the user with the most robust analysis of overall trends in climate (IPCC-TGICA, 2007; Tebaldi and Knutti, 2007). Such an analysis ensemble enables a robust assessment or projection uncertainty, considering the variability in the global climate models, downscaling methods, and emission scenarios.

The purpose of this study is to illustrate the level of uncertainty associated with trend analysis on extreme weather frequency and intensity indices at the local scale to determine if reliable trends can be detected, and if so what are their ranges. This analysis was applied to a study area in Hamilton, Ontario and results will be useful in defining the nature of future climate conditions in the local scale in the region. A range of possible future greenhouse gas emission scenarios and uncertainties associated with producing localized climate projections based on downscaled global climate model projections were prepared. This information could provide a comprehensive picture of future climate trends and uncertainty that could be used as a "likelihood" factor within climate change assessments locally. This analysis can also provide valuable information to help guide the development of scenarios for use in process-based hydrological modeling studies in the region.

To achieve the stated goals of this study, the spatial and temporal trends in historical climate data in Hamilton and surrounding area were analyzed. An ensemble of future climate projections of temperature and precipitation in the region was constructed to analyse the trend and uncertainty of future climate projections using extreme climate indices. An ensemble of different climate model datasets was compiled and then compared with trends in extreme temperature and precipitation indices. Extreme indices of climate have been analyzed in another studies such as (Powell and Keim, 2015; Donat et al., 2014; Sillmann et al., 2013; Yao et al., 2013; Bürger et al., 2012; dos Santos et al., 2011; etc.). The general approach in these studies was to compare historical observed trends with modelled historical trends using statistical test and graphical analysis in order to evaluate the model datasets. The focus of the current study is similar, however a more localized scale is examined and there is an emphasis on comparison of multiple different downscaled datasets. Validation of each downscaled dataset independently to the observed records in terms of ability to replicate statistical properties is a part of this comparison, but equally important was understanding how these various downscaled datasets compare relative to one another in the future. Currently, no such comparison is available in the literature at the local scale in the Hamilton region in Ontario.

2. Study area

The study area is centered on the City of Hamilton, located in southern Ontario, Canada at the western extent of Lake Ontario. The geographic area analyzed for this research is the municipal boundary of the City of Hamilton, plus a 10 km buffer which includes the full jurisdiction of the Hamilton Conservation Authority (Fig. 1). Annual precipitation varies between 750 and 900 mm. In the northern regions, the average air temperature ranges approximately between −7 °C (in January) and 19 °C (in July); and in the lake and southern regions, it ranges between −3 °C (in January) and 21 °C (in July). Major physiographic features influencing the local climate are Hamilton Harbour, marking the northern limit of the city, and

Please cite this article in press as: Razavi, T., et al.. Climate Risk Management (2016), http://dx.doi.org/10.1016/j.crm.2016.06.002

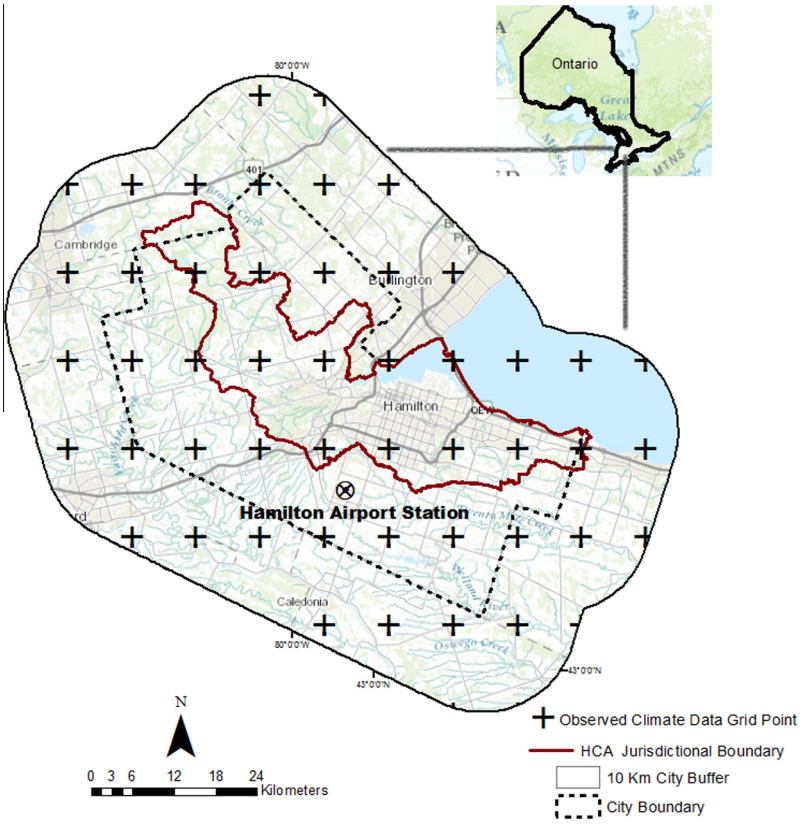

Fig. 1. Map of the study area showing the administrative boundary of the City of Hamilton and the Hamilton conservation area (HCA), along with the 10 km surrounding area.

the Niagara Escarpment running through the middle of the city across its entire breadth, dividing the city into "upper" and "lower" zones. The minimum elevation in the study area, near the lake Ontario, is 50 m above sea level (masl), and maximum high point in the study area limit is 350 masl in the northern regions (City of Hamilton, http://map.hamilton.ca).

3. Methods and materials

3.1. Methodology

The basis for comparing the various downscaled datasets was three key criteria:

1. Whether downscaled datasets were successful in replicating historical trends detected in observational datasets (determined with the Mann-Kendall test).
2. Comparing the historical observed and modelled using standard model performance statistics e.g. RMSE and statistical tests.
3. Comparison of the downscaled datasets in the future period using graphical methods and statistical trend analysis (Mann-Kendall), and statistical tests comparing each dataset's probability distribution (Kolmogorov-Smirnov test) .

Ultimately these tests were useful in determining whether trends in extreme indices could be detected despite uncertainty associated with an ensemble of climate model projections was firstly to compare how each modelled dataset reproduced. The local datasets compared were the World Climate Research Program's Fifth Coupled Model Intercomparison Project Phase 5 (CMIP5); ensemble of global climate models that were downscaled using a statistical bias correction method, along with the CanRCM4 regional climate model from the Canadian Centre for Climate Modeling and Analysis (CCCMA) and an ensemble of PRECIS model developed by the Ontario Ministry of the Environment and Climate Change in partnership with the University of Regina (Table 1). Together, this array of datasets is an ensemble that represents a combination of driving global climate models, downscaling techniques and emission scenarios that cover a sufficient range of possible future scenarios.

Please cite this article in press as: Razavi, T., et al.. Climate Risk Management (2016), http://dx.doi.org/10.1016/j.crm.2016.06.002

Table 1
Summary of datasets used.

Dataset & description of use in study	Driving global climate model	Scenarios analysed	Spatial resolution	Source
Re-gridded CMIP5 ensemble: Contains 23 global climate models, each with several runs that have been regridded to a common grid. All members were used.	All available GCMs from CMIP5	RCP 8.5 and RCP 4.5	Daily ~140 km	Maurer et al. (2007), Brekke et al. (2013)
CanRCM4: Regional climate model containing one run that was used	CanESM2	RCP 8.5 and RCP 4.5	Daily – 40 km	CCCma
PRECIS Ensemble: Regional climate model ensemble containing 5 runs that were used	HadCM2	A2	Daily – 25 km	Wang and Gordon (2013); http://ontarioccdp.ca

In the first step of analysis, gridded climate station data values for the study area were extracted (96 grid cells), then spatial and temporal trend analysis of historical climate in the region were performed to identify climate zones within Hamilton (trend analysis procedures described in Section 3.1). For the observed climate data, an average of the 96 grids in the study area were used for the analysis. The climate model datasets were downscaled to the statistical characteristics of observed precipitation and mean temperature time series from this average of 96 grids. In the next step, time series data from climate model projections for the geographic domain under consideration were extracted. Temporal trend and uncertainty analysis of the raw precipitation and temperature outputs of climate models were performed to evaluate the future trend of climate in the region. Extreme climate indices were then calculated on both the historical observed and climate model projections (details in Section 3.2). A statistical bias-correction technique was applied on climate model outputs to adjust the frequency distribution of climate models outputs to observed data. This represents a simple form of statistical downscaling commonly used in the development of local climate projection datasets (Ines and Hansen, 2006). The observed climate data were obtained from average of 96 grids in Hamilton region. The efficiency of the bias-correction technique in adjusting the climate model outputs to observe data is evaluated and considering the efficiency of bias-correction technique, annual trend and uncertainty of extreme indices are analyzed.

3.2. Seasonal and annual long-term trend analysis

Trend analysis was performed using the Mann-Kendall non-parametric statistical test on the seasonal and annual long-term trend for the historical period (1950–2011) and the future period (2012−2100) of temperature and precipitation time series. The Mann-Kendall test (Mann, 1945; Kendall, 1955) statistically assesses if there is a linear or non-linear upward or downward trend of the variable of interest over time. Mann-Kendall is a non-parametric test, therefore no assumption on the distribution of time series is required, however, there are some key assumptions associated to this test such as the requirement for observations, obtained over time, to be independent and identically distributed that means a very long record and non-stationarity of the time series (Mann, 1945; Kendall, 1955). Considering the uncertainty that comes from possible violations of this test, we applied the test on long-term seasonal total and maximum precipitation and seasonal mean and maximum temperature.

3.3. Extreme climate indices

A subset of extreme climate indices recommended by the WMO CCl/WCRP/JCOMM Expert Team on Climate Change Detection and Indices (ETCCDI) are defined and described in detail by Zhang et al., 2011 used in different studies (e.gBürger et al., 2012; Sillmann et al., 2013, etc.) were used in this study (see http://www.climdex.org/indices for downloading the indices from a number of global datasets). In selecting these indices, we considered indices, which most describe the extreme values of relevance to a group of local stakeholders involved in climate change adaptation planning in the study area. For instance, the hottest or coldest day of a year, or the annual maximum 1 day or 5 day precipitation rates; and threshold indices, which count the number of days when a fixed temperature or precipitation threshold is exceeded, for instance, frost days or tropical nights; and percentile-based threshold indices, which describe the exceedance rates above or below a threshold which is defined as the 10th or 90th percentile derived from the 1961–1990 base period. The extreme climate indices used in this study are summarized in Table 2. A statistical bias-correction technique described in Section 3.3 was applied to the daily temperature and precipitation time series of each climate model. The annual trends of indices in 2020s, 2050s and 2080s were then compared with the observed trend in 1960s and 1990s to evaluate the potential trends.

3.4. Bias correction technique

The Bias correction technique, which is used in this study to adjust the frequency distribution of all climate models to the observed data, was adopted from Ines and Hansen, 2006 and Samuel et al., 2012 for bias-correcting daily precipitation and temperature.

Please cite this article in press as: Razavi, T., et al.. Climate Risk Management (2016), http://dx.doi.org/10.1016/j.crm.2016.06.002

Table 2
Climate Extreme Indices (a subset of Core Set of Indices Recommended by the ETCCDI) used for this study.

Label	Index name	Definition	Unit
TXx	Max TX	Let TXx be the daily maximum temperatures in month k, period j. The maximum daily maximum temperature each month is then: $TXx_{kj} = \max(TXx_{kj})$	°C
TXn	Min Tn	Let TXn be the daily maximum temperature in month k, period j. The minimum daily maximum temperature each month is then: $TXn_{kj} = \min(TXn_{kj})$	°C
TNx	Max TN	Let TNx be the daily minimum temperatures in month k, period j. The maximum daily minimum temperature each month is then: $TNx_{kj} = \max(TNx_{kj})$	°C
TNn	Min TN	Let TNn be the daily minimum temperature in month k, period j. The minimum daily minimum temperature each month is then: $TNn_{kj} = \min(TNn_{kj})$	°C
FD	Frost days	Let TN be the daily minimum temperature on day i in period j. Count the number of days where TNij < 0 °C	Days
ID	Ice days	Let TX be the daily maximum temperature on day i in period j. Count the number of days	Days
SU	Summer days	Let TX be the daily maximum temperature on day i in period j. Count the number of days where TXij > 25_C	Days
TR	Tropical nights	Let TN be the daily minimum temperature on day i in period j. Count the number of days where TNij > 20 C	Days
RX1day	Max 1 day	Precipitation Let PR_{ij} be the daily precipitation amount on day i in period j. The maximum 1 day value for period j are: RX1dayj = max (PRij)	mm
RX5day	Max 5 day Precipitation	Let PR_{kj} be the precipitation amount for the 5 day interval ending k, period j. Then maximum 5 day values for period j are: $RX5day_j = \max(PR_{kj})$	mm
SDII	Simple daily intensity	Let PR_{wj} be the daily precipitation amount on wet days, PR ⩾ 1 mm in period j. If W represents number of wet days in j, then: $SDII_j = SDII_j = (\sum_{w=1}^{W} PR_{wj)/W}$	mm
R10mm	Heavy precipitation days	Let PR_{ij} be the daily precipitation amount on day i in period j. Count the number of days where PR_{ij} ⩾ 10 mm	Days
R20mm	Very heavy precipitation	Let PR_{ij} be the daily precipitation amount on day i in period j. Count the number of days where PR_{ij} ⩾ 20 mm	Days
CDD	Consecutive dry days	Consecutive wet days Let PRij be the daily precipitation amount on day i in period j. Count the largest number of consecutive days where PRij < 1 mm	Days
CWD	Consecutive wet days	Let PRij be the daily precipitation amount on day i in period j. Count the largest number of consecutive days where PRij ⩾ 1 m	days
R95p	Very wet days	Let PR_{wj} be the daily precipitation amount on a wet day w (PR ⩾ 1 mm) in period i and let PR_{wn95} be the 95th percentile of precipitation on wet days in the 1961–1990 period. If W represents the number of wet days in the period, then $R95_{pj} = \sum_{w=1}^{W} PR_{wj}$ where $PR_{wj} > PR_{wn95}$	mm
R99p	Extremely wet days	Let PR_{wj} be the daily precipitation amount on a wet day w (PR ⩾ 1 mm) in period i and let PR_{wn99} be the 95th percentile of precipitation on wet days in the 1961–1990 period. If W represents the number of wet days in the period, then: $R99_{pj} = \sum_{w=1}^{W} PR_{wj}$ where $PR_{wj} > PR_{wn99}$	mm
PRCPTOT	Total wet-day precipitation	Let PRij be the daily precipitation amount on day i in period j. If I represents the number of days in j then $PRCPTOT_j = \sum_{n=1}^{I} PR_j$	mm

3.5. Bias correction for precipitation

This method works by removing bias from the precipitation frequency and density distribution for each of the 12 months of future climate model data according to observed historical values, separately. Correcting any of these two precipitation components (frequency and density) will also correct the monthly total precipitation. To correct the frequency of precipitation of each month, the empirical distribution of the raw daily climate model was truncated above a threshold value. The threshold value (Xtr) was compute for each month using Eq. (1):

$$Xtr = F_{RCM}^{-1}(F_{obs}(\tilde{X})) \tag{1}$$

where F and F^{-1} indicate cumulative distribution function (CDF) and its inverse. The minimum observed precipitation amount ($\tilde{X}$) for a day to be considered as wet is 1 mm. To correct the precipitation intensity a two-parameter gamma distribution was fit to the truncated daily climate model and observed precipitation for each month. Then the CDF of the truncate daily climate model precipitation was mapped to the CDF of the observed and finally the corrected model precipitation on day i was calculated by substituting the fitted gamma CDFs into the following equation:

$$x_i' = \begin{cases} F_{I,obs}^{-1}(F_{I,RCM(Xi)}), & x_i \geqslant \tilde{x}, \\ 0, & x_i < \tilde{x}, \end{cases} \tag{2}$$

where x_i' is the bias-corrected precipitation value and $F_{I,RCM(Xi)}$ is the CDF of daily rainfall intensity above calibrated threshold X_{tr} and $F_{I,obs}$ is the observed data distribution. The equal time periods of 30-years future and historical climate projections and historical observed time series described earlier are used, herein.

3.6. Bias correction for temperature

The procedure is similar to precipitation bias correction but without any frequency correction and using a normal distribution instead of the gamma distribution. Similarly, daily climate model temperature distribution is mapped onto

the observed distribution for each of the 12 calendar months. The CDF of normal temperature distribution was first calculated for observed and model data, then climate model data are mapped on to the observed data. Similar to precipitation, equal periods of historical and future projections of observed and climate models were used in the equations.

3.7. Historical observed climate datasets

Historical daily precipitation, minimum temperature (Tmin) and maximum temperature (Tmax) observation records from 1950 to 2011 were obtained from following two sources (see Fig. 1):

1. Hamilton Airport Weather Station (1950–2011) (Environment Canada, 2014); and
2. The gridded historical weather data set from the McKenney et al., 2011 developed by the Natural Resources Canada and Environment Canada at 0.0833 degree grid resolution (approx. 8–10 km). These gridded climate data are derived from spatially and temporally interpolated daily temperatures and precipitation from Environment Canada weather stations over the 1951–2011 period. In total 96 grids were located in study area.

3.8. Climate models

Three distinct future climate model datasets were used in this analysis in order to compare a variety of climate forcing scenarios and downscaling techniques. These datasets included 83 raw re-gridded global climate model outputs from an ensemble of 36 GCMs used in the Fifth Coupled Model Intercomparison Project (CMIP5), a run from the CanRCM4 regional climate model, and a 3-member ensemble from the PRECIS regional climate model. The CMIP5 ensemble and CanRCM4 run were driven by two Representative Concentration Pathway (RCP) scenarios, representing radiative forcing of 4.5 W/m^2 (RCP4.5) and 8.5 W/m^2 (RCP8.5). The PRECIS ensemble was driven by the Special Report of Emission Scenarios' (SRES) A2 GHG emission scenario, representing a future of high emissions. The SRES and RCP emission scenarios were derived in different ways and are therefore not directly related, however Rogelj et al. (2012) and Stocker (2013) have compared these different vintages of scenarios. Evident from this comparison is the fact that RCP8.5 and SRES A2 have similar trends and magnitudes of radiative forcing, which ultimately result in similar, although not identical, ranges of global atmospheric warming. Table 1 provides a summary of the datasets employed and Section 3.8.1 through 3.8.3 contains additional detail.

3.8.1. The fifth phase of coupled model intercomparison project (CMIP5)

The Fifth Assessment Report (AR5) of the Intergovernmental Panel on Climate Change (IPCC) made use of a new set of greenhouse gas emission scenarios and new generation of GCMs produced through the Fifth Coupled Model Intercomparison Project (CMIP5) (Taylor et al., 2012).

The Climate and Hydrology Projections archive produced by the U.S. Department of the Interior's Reclamation Bureau (http://gdodcp.ucllnl.org/downscaled_cmip_projections/dcpInterface.html) contains a series of different downscaled climate projections over the contiguous United States (U.S.) and southern Canada using two downscaling techniques: (1) monthly Bias Correction and Spatial Disaggregation, and (2) daily Bias Corrected and Constructed Analogues. Additionally, this dataset has raw re-gridded GCMs output from all models and runs used in the CMIP5 ensemble. This latter dataset was used by extracting the time series for the three grids closest to Hamilton Airport station and subsequent Inverse Distance Weighted (IDW) weighting. The official model and group names of this archive are given in Appendix A. Combination of GCMS (access1-0, bcc-csm1-1, canesm2 – r1) and different number of runs and two scenarios of RCP 4.5 (moderate forcing emission scenario) and RCP 8.5 (high forcing emission scenario) from the ensemble were used in this study. The purpose of using this dataset was to capture a large range of projections associated with the global climate model ensemble, subsets of which are used in local downscaling.

3.8.2. CanRCM4

The Canadian Center for Climate Modelling and Analysis (CCCma) has developed a number of climate models to study climate change and variability and to understand the various process, which govern the climate system, and to make quantitative projections of future long-term climate change. The Canadian regional climate model (CanRCM4) is driven by the second generation of Canadian earth system model (CanESM2). RCP 4.5 and RCP 8.5 scenarios of this model are used in this study.

3.8.3. PRECIS modeling system

Ministry of Environment and Climate Change of Canada generated 5-member PRECIS ensemble modeling dataset. HadCM3 (developed by Hadley Centre of Met Office, United Kingdom model) was dynamically downscaled to resolution of 25 km × 25 km (Wang and Gordon, 2013) driven by different boundary conditions (i.e. HadCM3Q0, Q3, Q10, Q13, and Q15). The statistics (percentiles and averages) of climate data including precipitation and maximum/minimum temperature are available at the Ontario Climate Change Data Portal (OCCDP, http://www.ontarioccdp.ca/). In this study three outputs from PRECIS ensemble dataset were used. Given the analysis required, the raw time series outputs were used, as opposed to the percentiles.

Please cite this article in press as: Razavi, T., et al.. Climate Risk Management (2016), http://dx.doi.org/10.1016/j.crm.2016.06.002

4. Results and discussion

4.1. Historical observed trends

The observed historical climate for the variables of annual total and maximum precipitation and annual mean and maximum temperature for the period of 1950–2011 are shown in Fig. 2. These datasets represent the basis for calculation of the extreme indices and therefore exploring them to determine what trend can be elucidated is an important first step in understanding the overall climatic trends and baseline variability in the region. It is largely this variability that is used to characterize uncertainty in climate over the historical period.

Evident in Fig. 2 is the fact that the two historical datasets explored (gridded versus station observations) differ in how they capture extreme events. The gridded historical dataset tends to mute the extreme values captured in the station-based data. This is not unexpected, as the gridded data, even for any given cell in the region, represents a weighted-average based on the spline technique used in the development of the gridded dataset as is described in McKenney et al. (2011). From a graphical analysis of Fig. 2, it is also evident that the extreme values recorded in the station data are at the upper end, if not exceeding the spatial variability associated with the gridded data. Fig. 2 also shows the range of spatial variability in temperature and precipitation in the region. For example, the difference between the grid with lowest and highest annual total precipitation is approximately 100 mm and this range for mean annual temperature is 2 °C. This range can be considered significant, but does likely reflect key physical processes that influence the climate locally in the study area. According to Fig. 3, the average of historical total precipitation near the Lake Ontario has been less than that above the Niagara Escarpment and western regions where there is a higher elevation. Higher maximum 1-day precipitation was also recorded closer to the lake and mountain region compared to western area. Mean annual and maximum temperature were higher near the lake and in south part and lower in northern area with high elevation.

Seasonal and annual total, maximum 1-day and 5-day precipitation, mean and max seasonal temperature values are evaluated in terms of significant trend using Mann-Kendall test and the results are presented in Table 3. This analysis suggests that at 5 percent significance level increasing trends in total annual and seasonal precipitation in Winter (DJF), Spring (MAM), and Summer (JJA) were detected using the station data. Statistically significant annual and seasonal temperature increases in Fall (SON) were detected in both the gridded dataset and the station data. Consistent with the graphical analysis is the fact that statistical tests showed significant results more frequently in the station data compared to the gridded dataset. Based on the analysis offered from Figs. 2 and 3 and Table 2, it is evident that while gridded historical datasets offer a very useful product for understanding spatial variability and its contribution to uncertainty in climatic trends, it is important to acknowledge that these datasets may consistently underestimate the extremes actually experienced at the local scale.

4.2. Trends in climate model datasets

Daily temperature and precipitation time series were extracted for the climate model dataset grids closest to Hamilton Airport station using CMIP5 and CanRCM4, then Inverse Distance Weighted (IDW) average were calculated. For the PRECIS dataset, three runs of the grid cell containing Hamilton airport station were collected and analyzed. The annual total precipitation, maximum 1-day precipitation, mean and maximum temperature for each climate data set in its projection period are demonstrated in comparison with the observed climate data obtained by averaging the 96 grid values inside the area in Figs. 4–6. We used the gridded instead of station dataset to account for the geographic variability in the whole study area and minimize the difference between the spatial resolution of observation and climate models. The climate model datasets in Figs. 4–6 are not yet bias-corrected in order to analyse the influence of the raw datasets on finding the trend.

Fig. 4 illustrates annual total/mean and maximum values of precipitation and temperature for all the individual models in CIMP5 ensemble used in this study (83 members) along with its 10th and 90th percentiles (uncertainty bounds) in the projection time frame (1950–2098). For annual total precipitation and maximum 1-day precipitation, the two scenarios of RCP 4.5 and RCP 8.5 have very similar pattern and boundaries. Observed total precipitation lies in the lower boundary (between the median and 10th percentile) of the historical modelled data for both scenarios while observed maximum 1-day precipitation lies in the lower and upper limits of the ensemble. For annual mean temperature the observed and modelled values tend to demonstrate agreement, with the median of the ensemble historical models for both scenarios. The increasing trend for annual total precipitation and mean temperature for both scenarios is visible from the graphs especially for annual mean and maximum temperature, and these results are consistent with those of the Mann-Kendall test results (Table 4) that found significant increasing trend for annual mean and maximum temperature and total precipitation predicted by average of CIMP5 ensemble.

Fig. 5 shows the total and maximum annual precipitation and mean and maximum annual temperature values from CanRCM4 model in its projection time period (1950–2100). For annual total and maximum 1-day precipitation the historical modelled and observed values have generally good agreement except for peak values which historical model has sharper peaks and for future projection RCP 8.5 scenario indicate sharper peak values compared to RCP 4.5. For mean and maximum annual temperature, the historical modelled temperature is higher than the observed by approximately 3 °C for the annual mean and 8 °C for annual maximum temperature. Annual mean and maximum temperature using this model indicate an increasing trend, which is in line with Mann-Kendall test results (Table 4).

Please cite this article in press as: Razavi, T., et al.. Climate Risk Management (2016), http://dx.doi.org/10.1016/j.crm.2016.06.002

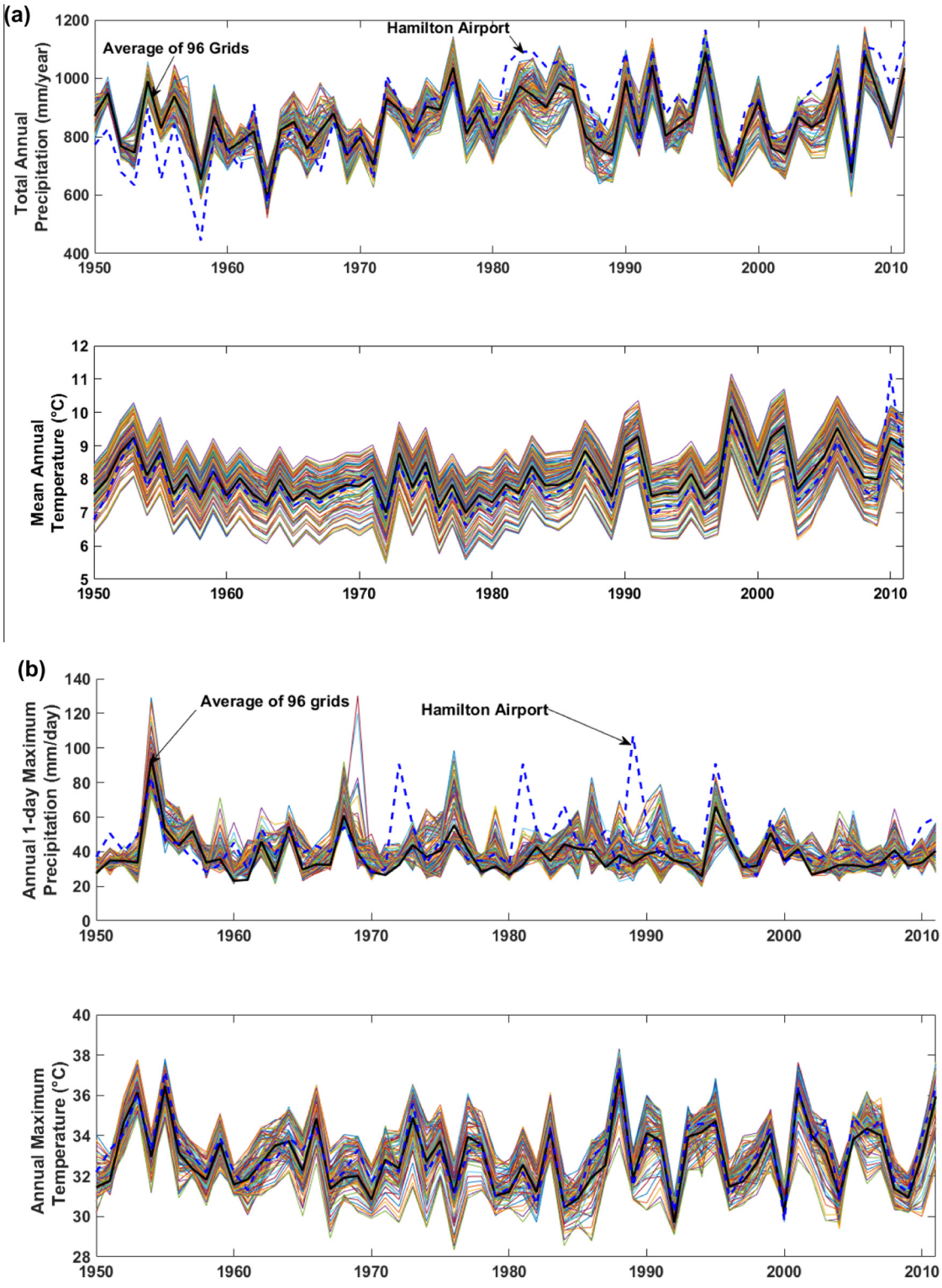

Fig. 2. Historical temperature and precipitation temporal trend in Hamilton region using CANGRD data set (black thick line is the mean).

Fig. 6 shows the annual precipitation and temperature values using three members of PRECIS ensemble modeling system in its projection time period (1960–1990, 2015–2095). Observed annual total precipitation lies in the range of historical modelled values of three ensemble members while observed annual 1-day maximum precipitation is lower than the

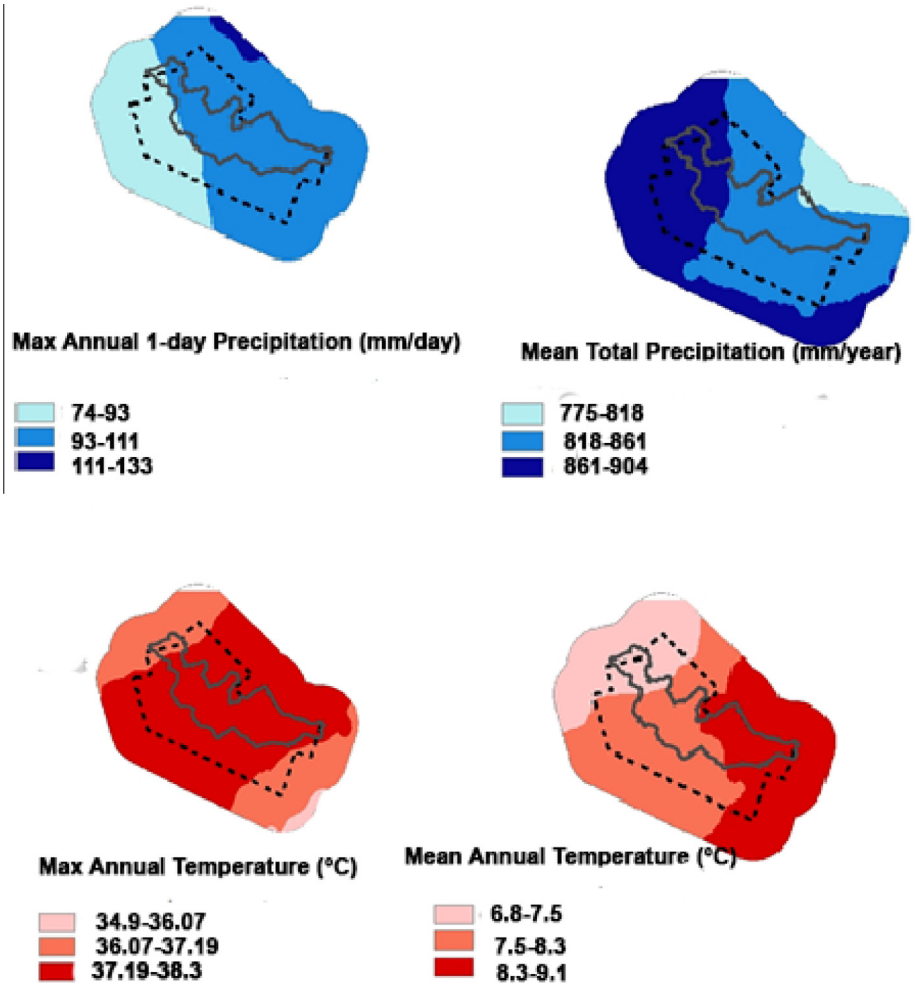

Fig. 3. Spatial pattern of historical precipitation and temperature (1950–2011) using gridded observed climate data (McKenney et al., 2011) in Hamilton region (Schematic maps).

Table 3
Seasonal and Annual long-term trend analysis result of historical climate data (1950–2011) using Mann-Kendall test at 5 % significance level.

Variable	Historical datasets	Seasonal trends				Annual trends
		Winter (DJF)	Fall (SON)	Sumer (JJA)	Spring (MAM)	
Total precipitation (mm)	McKenney et al. (2011)	No trend	No trend	No trend	No trend	No trend
	Hamilton Airport Station	Increasing	Increasing	Increasing	No trend	Increasing
Max 1-day precipitation (mm/day)	McKenney et al. (2011)	No trend	No trend	No trend	No trend	No trend
	Hamilton Airport Station	No trend	No trend	No trend	No trend	No trend
Max 5-day precipitation (mm/day)	McKenney et al. (2011)	No trend	No trend	No trend	No trend	No trend
	Hamilton Airport Station	No trend	No trend	No trend	No trend	No trend
Mean temperature (°C)	McKenney et al. (2011)	No trend	No trend	No trend	Increasing	Increasing
	Hamilton Airport Station	No trend	No trend	No trend	Increasing	Increasing
Max temperature (°C)	McKenney et al. (2011)	No trend	No trend	No trend	No trend	No trend
	Hamilton Airport Station	No trend	No trend	No trend	No trend	No trend

historical modelled values. Observed annual mean and maximum temperature are generally lower than the three historical modelled values while one of the ensemble members indicates unusual high values that cause some inhomogeneities. This problem might be due to the wrong initial values or restart problems for this particular PRECIS run. Mann-Kendall test performed on future projection of annual total and maximum precipitation and annual mean and maximum temperature at 5% significance level (Table 4) suggest that in the long term future period (~2012–2100) scenario RCP 8.5 of CanRCM4 and

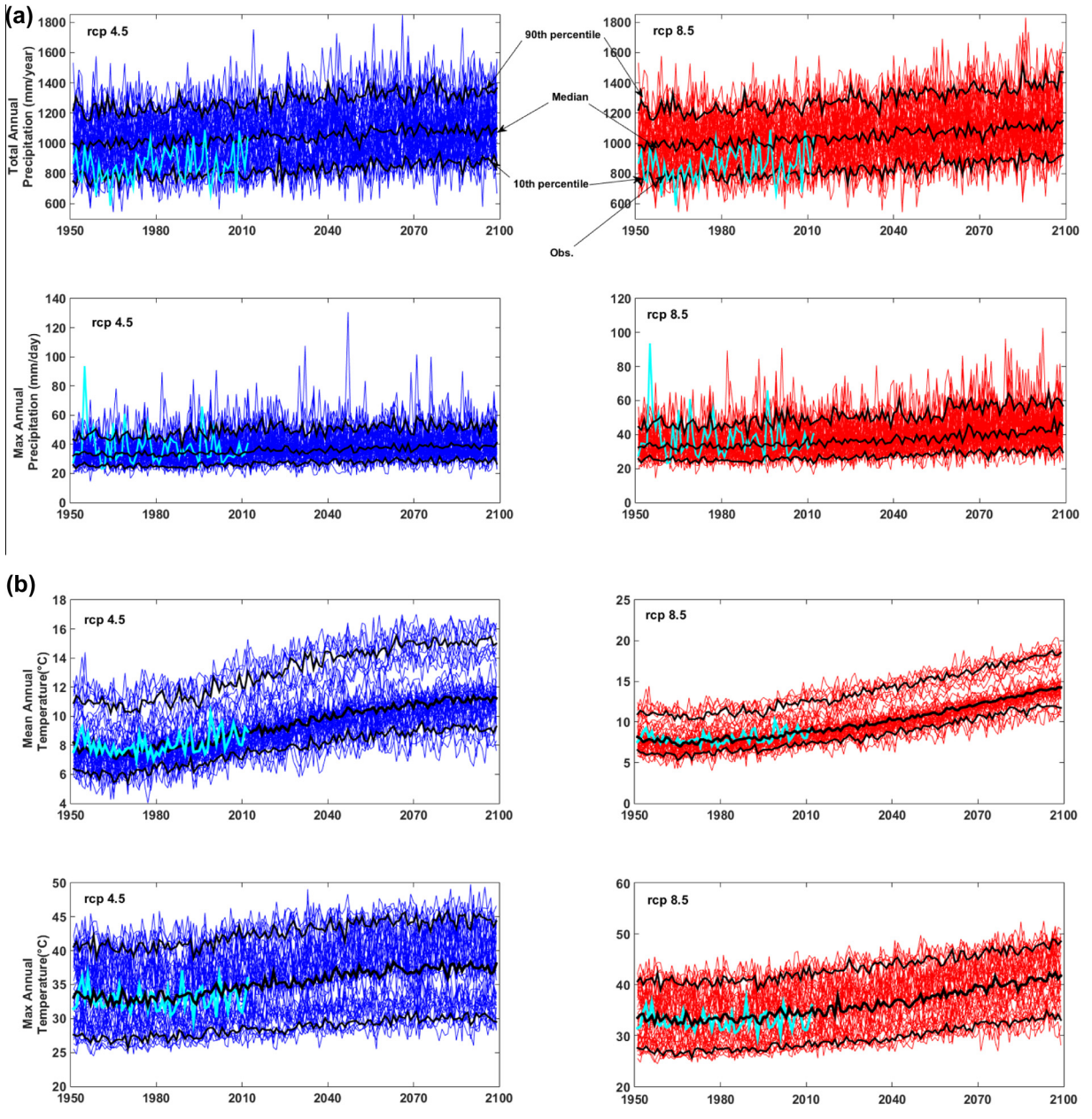

Fig. 4. Annual temperature and precipitation trend using CMIP5 ensemble with uncertainty bounds (10th and 90th percentiles – black marginal lines) and observed climate data (light blue line) obtained from CANGRD data set. (For interpretation of the references to colour in this figure legend, the reader is referred to the web version of this article.)

average of the CIMP5 ensemble for both scenarios predict significant increasing trend of annual total precipitation. For 1-day and 5-day maximum precipitation, only average of CIMP5 ensemble predicts increasing trend while for mean and maximum annual temperature all climate models predict significant increasing trend.

4.3. Influence of bias correction on climate models data sets

Due to different grid size of observed and climate models, and since there are differences between the historical model and observed time series in the annual precipitation and temperature trends (Figs. 4–6), the bias correction technique described earlier is applied to the daily precipitation and temperature time series of climate models to adjust their frequency and distribution to the gridded observed time series. Statistical bias-correction is usually used in local climate change impact studies such as hydrologic modeling or trend analysis to adjust for scale difference between climate models and observed

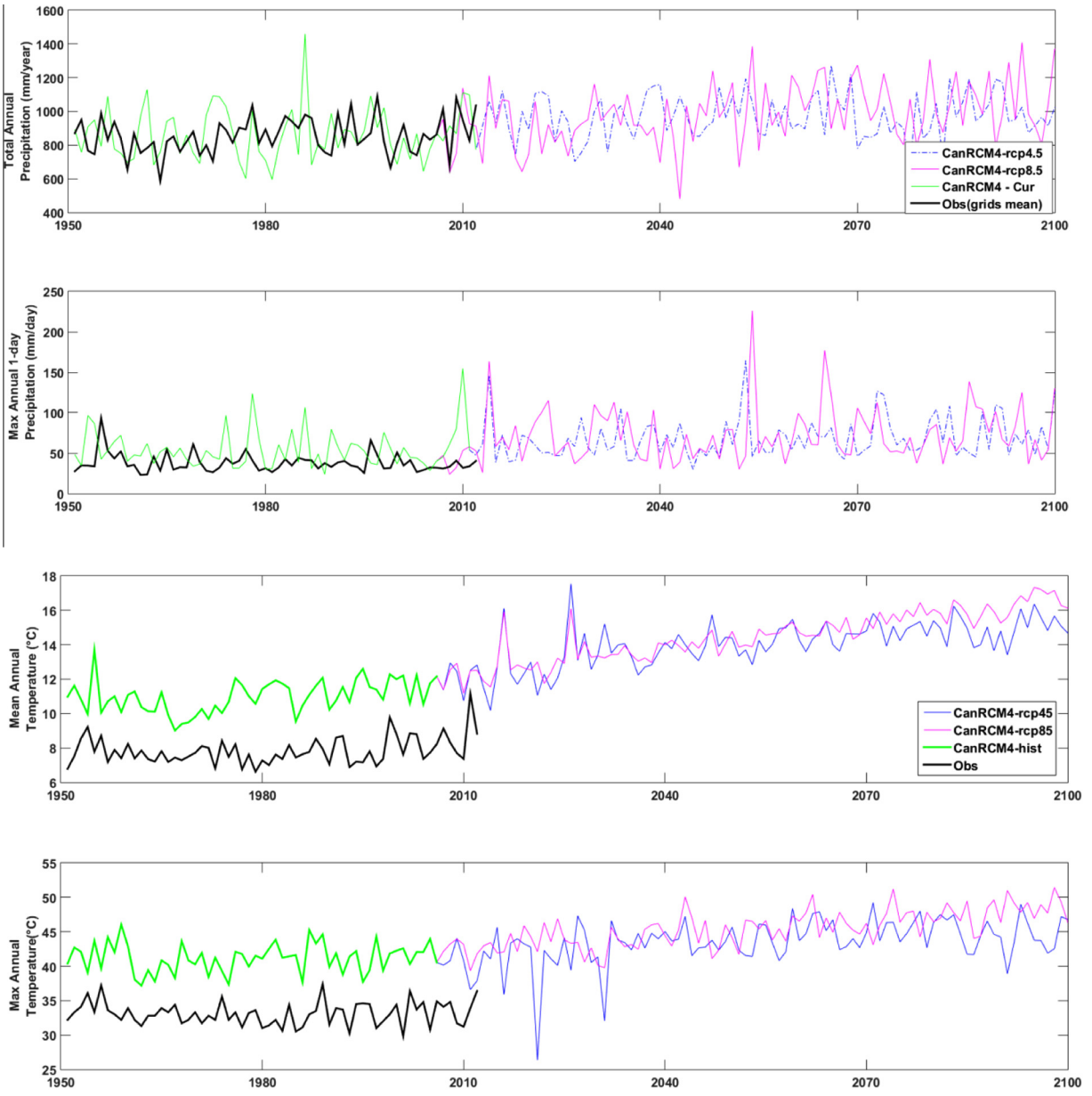

Fig. 5. Annual precipitation and temperature trend using CANRCM4 model – Observed climate data obtained from CANGRD data set (black lines are the observed graphs).

climate data from stations or gridded products (e.g., Sharma et al., 2007; Samuel et al., 2012; Bürger et al., 2012). Although bias correction effectively reduces the statistical error present in the raw climate model datasets, this does not necessarily mean that users should place greater confidence in the accuracy of that information (Ehret et al., 2012). Bias correction is essentially a mathematical procedure to render the dataset more statically consistent with the observed data, and essentially amounts to "calibration" of the model results after the fact. The errors removed through bias-correction are the result of the way physical processes are captured in the original climate models, their boundary and initial conditions, the large spatial scale of grid cells, and the effects of the numerical algorithms used for solving the partial differential equations within the model. These can be considered fundamental sources of uncertainty that bias correction accounts for, but which do not necessarily make results more accurate or precise. The aim of applying bias-correction in this study was to evaluate the influence of bias correction on climate model downscaling and account for the uncertainty introduced through its application.

Another potential consideration when using bias correction relates to the coherence between climate variables. Many statistical downscaling and bias-correction methods are applied independently to different climate variables, while

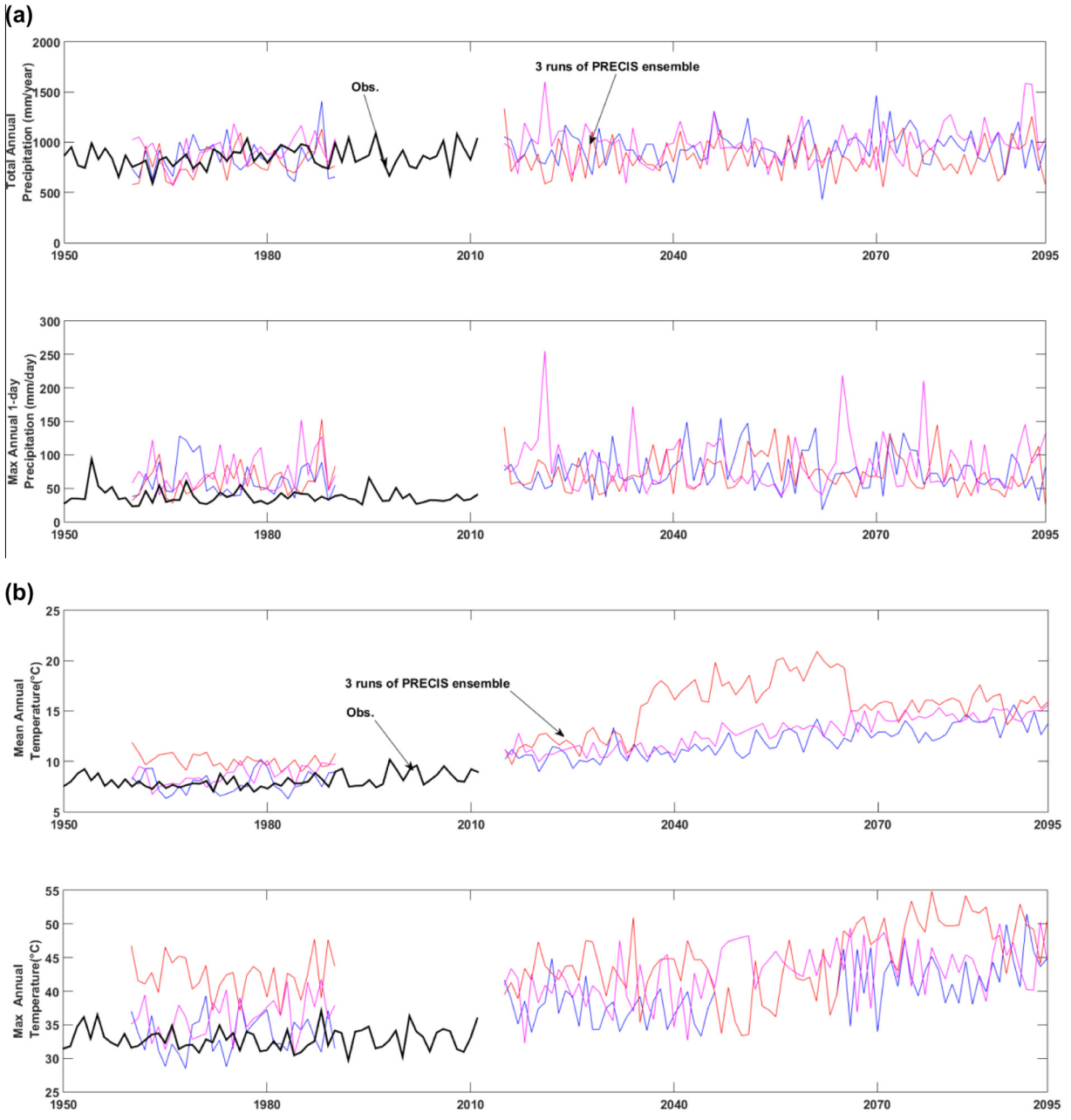

Fig. 6. Annual precipitation and temperature trend using 3 runs of PRECIS ensemble model – Observed climate data obtained from CANGRD data set (black lines are the observed graphs).

Table 4
Mann-Kendall test results at 5% significance level for future projection of annual precipitation and temperature.

Variable & scenario	Average CIMP5 (2012–2098)		CanRCM4 (2012–2100)		Average PRECIS (2015–2095)
	RCP 4.5	RCP 8.5	RCP 4.5	RCP 8.5	A2
Total precipitation (mm/year)	No trend	Increasing	Increasing	Increasing	No trend
Max. 1-day precipitation (mm/day)	No trend	No trend	Increasing	Increasing	No trend
Mean temperature (°C)	Increasing	Increasing	Increasing	Increasing	Increasing
Max. temperature (°C)	Increasing	Increasing	Increasing	Increasing	Increasing

Please cite this article in press as: Razavi, T., et al.. Climate Risk Management (2016), http://dx.doi.org/10.1016/j.crm.2016.06.002

dynamical climate models are able to represent the relationships among them in a physically based manner where laws related to the conservation of mass, energy and momentum are preserved. By downscaling or bias-correcting dynamic model outputs, the physical relationships within the earth-atmosphere system may no longer be preserved. The implication would be that the resultant variables could be inconsistent with one another, and potentially physically implausible (e.g., rainfall when humidity, temperature and pressure wouldn't otherwise line-up to produce precipitation).

To compare the effect of bias-correction on the climate model datasets, statistical tests of Kolmogorov-Smirnov, and RMSE of extreme climate indices were conducted on the datasets before and after bias correction with respect to historical observed indices. Results of the Mann-Kendall test applied to the corrected and uncorrected datasets were also compared. The Kolmogorov-Smirnov test (Table 5) indicates that the historical annual total precipitation obtained from all climate models had similar probability distribution to the observed historical values. The variables of maximum 1-day for all the climate model datasets did not have the same probability distribution as the observed record. For the CMIP5 ensemble average, probability distributions were the same only after bias-correction was applied. For the annual mean and maximum temperature, the probability distribution of the climate models values before bias-correction were not similar to the observed values but they became similar after bias-correction except for scenario 4.5 of CIMP5 ensemble. These results indicate that the statistical bias-correction had a greater influence on the temperature time series compared to precipitation time series. This is consistent with the graphical analysis of the climate model time series before bias-correction compared to observed historical time series in Figs. 4–6.

Mann-Kendall test results (Table 6) indicate no significant trend in annual total and maximum precipitation of observed and climate models before and after bias-correction. For annual mean temperature, this test indicates a significant increasing trend for historical observed and climate models, before and after bias-correction, for annual maximum temperature no significant trends in historical observed data sets were detected, but all the climate models simulate increasing trends before and after bias-correction. Only CanRCM4 did not indicate any significant trends for annual maximum temperature. These results indicate that the applied statistical bias-correction does not change the increasing or decreasing trend for almost all major annual climate extreme indices. The RMSE between indices of climate models obtained before and after bias correction and the indices of observed values for historical period of 1950–2010 for CanRCM4 and CIMP5 ensemble and 1960–1990 for PRECIS model runs are presented in Table 7. For each member of the CIMP5 ensemble the RMSE was calculated separately and the mean was finally calculated. These results show that bias correction did reduce the RMSE value of extreme indices of temperature values such as TXx, substantially, but for precipitation indices of CanRCM4 it didn't reduce the RMSE values and for the CIMP5 ensemble it reduced RMSE values slightly. For three runs of PRECIS, the RMSE values of both precipitation and temperature indices were improved after bias-correction.

This analysis indicates that the applied statistical bias correction can adjust the temperature data to the observed data set more effectively compared to the precipitation data. This is also evident from Kolmogorov-Smirnov test results (Table 5) that indicates the probability distribution of annual mean and maximum temperature become similar to the observed data after bias-correction. For precipitation, the RMSE values did not show as much difference and this can also be verified by the Kolmogorov-Smirnov test that indicates the probability distribution of annual total and maximum precipitation did not change after bias correction (Table 5).

4.4. Trends in extreme climate indices over various periods

Temperature and precipitation extreme indices were calculated for 1951–2100 period, evaluated annually, and in time periods of 30-years for observed historical and climate models in their projection periods, representing the typical normal periods used in climate change risk assessment and planning. Observed climate indices of the 1990s (1981–2010) were compared with the observed indices of 1960s (1951–1980) to determine whether historical trends found from the Mann-Kendall test were also detected when normal period statistics are compared. The indices for the future projection periods of the 2020s (2011–2040 for CanRCM4 and CIMP5 and 2015–2040 for PRECIS), 2050s (2041–2070 for CanRCM4, CIMP5 and PRECIS), and 2080s (2071–2100 for CanRCM4, 2071–2098 for CIMP5 and 2071–2095 for PRECIS) were also compared to the observed ones of 1990s.

The trend of annual extreme indices in observed data (average of 96 grids) and future projection of climate models are presented in Figs. 7 and 8. In Fig. 7, the bias-corrected temperature indices of all climate models are plotted and for precipitation indices in Fig. 8, the bias-corrected precipitation indices of PRECIS and the CIMP5 ensemble and the non-bias-corrected indices of precipitation for CanRCM4 (considering RMSE values in Table 7) are plotted. Table 8 presents the observed indices of 1990s and 1960s and future projections of indices by climate models in 2020s, 2050s, and 2080s before and after bias-correction. Table 9 presents the 10th and 90th percentile uncertainty bound of future model projections of bias corrected and non-bias corrected climate indices. According to Table 8 bias corrected and non-bias corrected indices, reveal similar increasing or decreasing trend for most of the indices in historical period of 1990s compared to 1960s. This is in line with the results of Mann-Kendall test for annual indices (Table 6). This analysis shows annual maximum of maximum temperature (TXx) indicates increasing trend over all future normal periods compared to the current period. The observed annual TXx in 1990s increased by +0.63 °C (insignificant increase) compared to observed equal value of 1960s, and from the bias corrected indices it can be seen that median index of the CIMP5 ensemble, CanRCM4 and mean index of PRECIS predicted an increase of maximum +2.4, +1.4, and +4.6 °C in 2020s and +5.4, +3.6, +6 °C in 2050s and +7.7, +4.6, and +8 °C, respectively, compared to the observed historical period of 1990s. Furthermore, Table 9 reveals that TXx is

Please cite this article in press as: Razavi, T., et al.. Climate Risk Management (2016), http://dx.doi.org/10.1016/j.crm.2016.06.002

Table 5
The Kolmogorov-Smirnov test results at 5% significance level.

Variable	Before bias correction					After bias correction				
	Average* of CIMP5 ensemble		CanRCM4		Average of PRESIC ensemble	Average of CIMP5 ensemble		CanRCM4		Average of PRESIC ensemble
	rcp 4.5	rcp 8.5	rcp 4.5	rcp 8.5	A2	rcp 4.5	rcp 8.5	rcp 4.5	rcp 8.5	A2
Annual total precipitation (mm)	Sim.	Sim.	Sim.	Sim.	Sim.	Sim.	Sim.	Sim.	Sim.	Sim.
Annual Max 1-day precipitation (mm/day)	Non-sim.	Non-sim.	Non-sim.	Non-sim.	Non-sim.	Sim.	Sim.	Non-sim.	Non-sim.	Non-sim.
Annual Mean temperature (°C)	Non-sim.	Non-sim.	Non-sim.	Non-sim.	Non-sim.	Non-sim.	Sim.	Sim.	Sim.	Sim.
Annual Max temperature (°C)	Non-sim.	Non-sim.	Non-sim.	Non-sim.	Non-sim.	Non-sim.	Sim.	Sim.	Sim.	Sim.

Notes: Sim. = Similar probability distribution based on results of the Kolmogorov-Smirnov test.
Non-sim. = Non_similar probability distribution based on results of the Kolmogorov-Smirnov test.
* The indices for each member of ensemble are first calculated and then the average is taken.

predicted to be in the range of 39.1–45.6 °C in 2020s, 40.8–47.8 °C in 2050s, and 41.1–48.1 °C in 2080s. Similarly, for minimum of maximum temperature (TXn), maximum of minimum temperature (TNx) and minimum of minimum temperature (TNn), the observed historical data of 1990s indicated increase of 1, 1.5, and 0.5 °C compared to 1960s and similarly all climate models predicted increasing trends for the 2020s, 2050s, 2080s as could be seen in Table 8. Observed mean annual number of Forest Days (FD) and Ice Days (ID) indicated decreasing trends and observed values of Summer Days (SU) and Tropical Nights (TR) indicated increasing trend over the historical period of 1990s compared to 1960s.

All climate models predicted decreasing trends of FD and ID and increasing trends of SU and TR in 2020s, 2050s and 2080s compared to current period of 1990s. Furthermore, for precipitation indices, observed maximum 1-day precipitation (RX1-day) increased by 5.1 mm in 1990s compared to 1960s and climate models predict the increase of 14.5–76.8 mm in 2020s, and increase of 10.3–98.3 mm in 2050s, and increase of 11.8–64.5 mm in 2080s. Observed maximum 5-day precipitation (RX5day) decreased by 11.3 mm in 1990s compared to 1960s but all climate models predicted increasing trends of RX5day in 2020s, 2050s and 2080s compared to 1990s. All climate models predict increase of R20mm by 1–3 days per year in 2020s, 2050s and 2080s. Maximum consecutive dry days (CDD) indicated decreasing trends from 1960s to 1990s and CIMP5 median predict that trend to continue, CanRCM4 and PRECIS however predicted increasing trend compared to 1990s. All climate models predict increasing trend for maximum Consecutive Wet Days (CWD) in 2020s, 2050s, and 2080s compared to 1990s. For R95p (very wet days) and R99p (extremely wet days) all climate models predict increasing trend in 2020s, 2050s and 2080s compared to 2020s. Annual total wet precipitation (PRCPTOT) demonstrated increasing trend in both historical observed from 1960s to 1990s and by all climate models during 2020s, 2050s and 2080s compared to 1990s.

Annual trend of extreme temperature indices in Fig. 7 demonstrate increasing trend TXx, TXn, TNn, TNx, TR, SU and decreasing trend of FD and ID over the long term period of 1950–2100, and the observed time series are within the uncertainty bounds of climate models prediction. This trend is in line with the detected trend from normal 30-year periods obtained from Table 8 and 9. Furthermore, annual trends of extreme precipitation in Fig. 8 demonstrate that for PRCPTOT, R 90p and R 20 mm there is an increasing trend detected in normal 30-year periods (Tables 8 and 9). For other precipitation indices such as RX1day, RX5day, CDD and CWD, the trend detected from normal 30-year periods is not significant or it's not consistent in terms of different observed historical and climate models future periods, and it cannot be visually detected from the plot. Additional discussion on the results of indices is provided in Section 4.5.

4.5. Implications of using downscaled datasets for understanding local impacts of climate change on extremes

Changes in climate extremes are of great interest to decision makers at the local scale because they imply shifts in the types of hazards that are often of greatest concern to communities (Cheng et al., 2012; IPCC, 2012). Despite the importance of changes in extreme climate, end-users are often challenged to determine the most appropriate climate model dataset for their purposes, with factors of information accuracy, uncertainty and ease-of-use/cost being primary factors. There are several critical challenges directly related to each of these factors however, that were revealed in the case study presented throughout this study, which will be explored further throughout this section:

1) Imprecision of downscaled climate model datasets;
2) Compounding of uncertainty due to inherent ambiguity about future emission scenarios; and
3) Added value to ease-of-use and cost of downscaling.

Table 6
Mann-Kendall test results at 5% significance level.

Variable	Before bias correction						After bias-correction				
	Obs.	Average of the CIMP5 ensemble		CanRCM4		Average of the PRESIC ensemble	Average of the CIMP5 ensemble		CanRCM4		Average of the PRESIC ensemble
		rcp 4.5	rcp 8.5	rcp 4.5	rcp 8.5	A2	rcp 4.5	rcp 8.5	rcp 4.5	rcp 8.5	A2
Annual total precipitation (mm)	No trend	No trend	No trend	No trend	No trend	No trend	No trend	No trend	No trend	No trend	No trend
Annual Max. 1-day precipitation (mm/day)	No trend	No trend	No trend	No trend	No trend	No trend	No trend	No trend	No trend	No trend	No trend
Annual Mean temperature (°C)	Increasing	Increasing	Increasing	Increasing	Increasing	Increasing	Increasing	Increasing	Increasing	Increasing	Increasing
Annual Max temperature (°C)	No trend	Increasing	Increasing	Increasing	Increasing	Increasing	Increasing	Increasing	No trend	No trend	Increasing

Please cite this article in press as: Razavi, T., et al., Climate Risk Management (2016), http://dx.doi.org/10.1016/j.crm.2016.06.002

Table 7
RMSE of annual climate indices calculated for historical climate model output and observed data, before and after bias-correction.

Extreme index	RMSE of climate indices before bias-correction					RMSE of climate indices after bias-correction				
	Can RCM4	CIMP5	PRECIS			Can RCM4	CIMP5	PRECIS		
		Mean	1	2	3		Mean	1	2	3
	1950–2010		1960–1990			1950–2010		1960–1990		
TXx	8.9	4.9	3.8	10.2	4.7	2.2	2.2	3.6	3.6	3.4
TXn	4.6	5.2	3.9	4.4	3.4	4.1	4.8	3.4	3.7	3.2
TNx	4.0	3.5	2.4	6.9	3.8	1.6	2.2	1.6	2.3	1.6
TNn	5.2	6.6	4.9	6.1	5.4	5.1	4.8	5.6	4.4	4.9
FD	37.7	20.6	14.2	18.5	16.0	14.7	15.9	14.1	11.8	13.2
ID	28.1	28.0	21.9	24.4	19.1	17.3	20.7	21.3	23.4	18.9
SU	54.1	32.8	20.6	28.8	13.6	19.2	18.7	17.5	18.1	12.1
TR	19.2	17.6	10.1	28.9	20.5	5.9	5.9	5.8	5.5	4.1
RX1day	27.5	34.3	31.6	30.4	41.8	28.9	33.2	22.0	22.6	24.0
RX5day	35.5	46.0	38.2	43.5	56.2	38.4	45.1	26.3	29.6	30.0
SDII	1.3	3.7	2.3	2.2	2.5	1.1	3.1	1.0	1.0	0.8
R10mm	7.3	26.2	8.0	7.7	7.5	7.6	25.0	9.1	7.2	7.0
R20mm	4.4	6.3	5.9	4.4	5.0	4.0	5.3	3.6	3.1	3.2
CDD	7.0	15.4	7.4	10.3	7.0	5.8	14.2	6.7	6.5	6.4
CWD	2.3	10.5	2.3	2.7	2.3	2.1	7.1	2.2	2.3	2.3
R95p	133.7	120.6	261.5	134.7	170.9	152.8	117.6	174.8	125.0	132.9
R99p	88.3	70.1	135.7	81.8	106.6	93.2	62.7	119.1	85.1	93.2
PRCPTOT	174.7	213.0	202.7	171.2	169.7	173.7	109.7	160.3	148.7	136.2

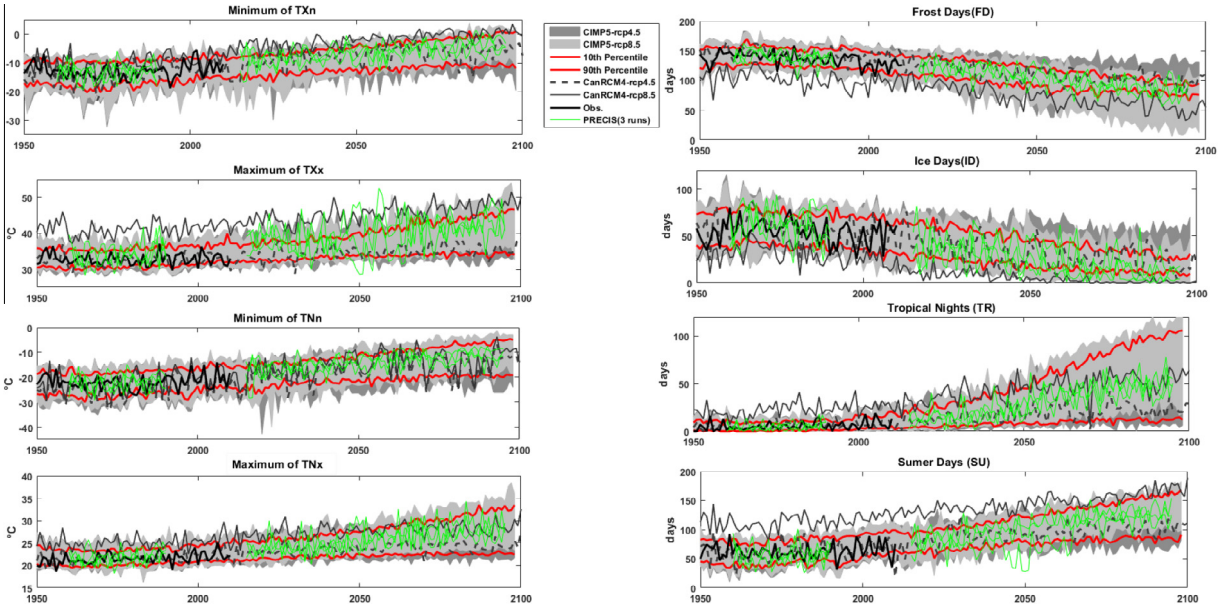

Fig. 7. Trend of extreme temperature indices calculated using CanRCM4, CIMP5 ensemble and PRECIS models and observed climate data of CANGRD (average of 96 grids) (black lines are the observed graphs).

At the local scale, downscaled climate model projections tended to be imprecise for both the historical and future periods, where they demonstrated great variability among datasets in the simulated values of extreme indices for any particular year. Generally, temperature-based indices exhibited less inter-dataset variability compared to precipitation indices over the historical period. That being said, individual datasets within the ensemble tended to agree with respect to the direction of trends for the extreme indices and in their overall variability compared with the historical record. Additionally, trends over the historical period were generally projected to continue into the future.

From a quantitative perspective however, the range of values shown among the climate model datasets in the historical period tended to exceed natural variability within that same timespan when examining the full range of values (min-max range of the CMIP5 ensemble) (Figs. 7 and 8). When removing outliers and looking at the 10–90th in the CMIP5 ensemble

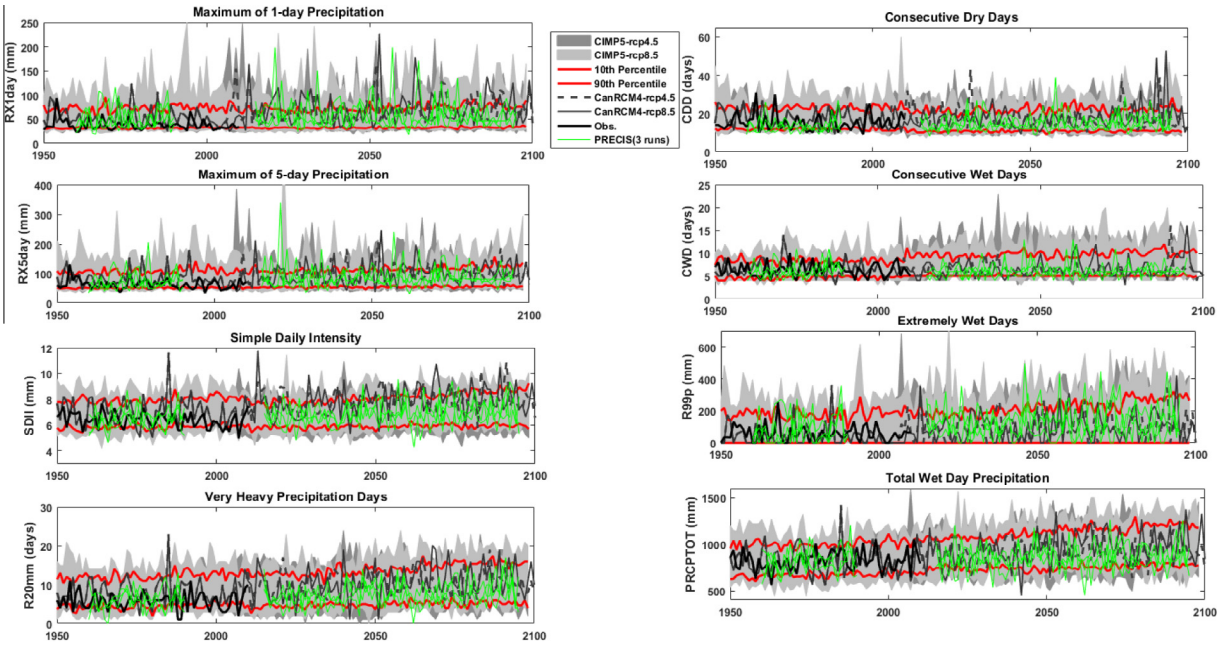

Fig. 8. Trend of extreme precipitation indices calculated using CanRCM4, CIMP5 ensemble and PRECIS models and observed climate data of CANGRD (average of 96 grids) (black lines are the observed graphs).

however, historical variability actually tended to approach or exceed these limits, indicating that this range can likely represent an accurate picture for the historical period. When comparing the two dynamically downscaled datasets of the PRECIS ensemble and CanRCM4 over the historical period, it is evident that the two tended to demonstrate similar ranges of variability as the 10th to 90th percentile range in the CMIP5 ensemble. It should be noted, however, that certain timespans within the historical period (e.g., 1990–2011) precipitation extremes for the observed and dynamically downscaled CanRCM4 tended to be at the low end of the CMIP5 ensemble. While this suggests that CanRCM4 did provide a more accurate representation of this variable, this may be a function of the bias correction and not necessarily the CanRCM4 model itself. This points to the fact that caution should be applied when relying on bias correction.

For the future periods, it is notable that the 10th–90th percentile range within the CMIP5 ensemble was almost identical as the range shown over the historical period. Among the dynamically downscaled datasets, the CanRCM4 model did consistently project values at the upper range of the CMIP5 ensemble while the PRECIS ensemble was more in-line with the CMIP5 mean. This difference may however be a function of different emission scenarios used (RCPs vs. A2). Nonetheless, guidance on climate model projections does suggest using as many possible scenarios as is feasible in an assessment (IPCC, 2014), and both A2 and RCP8.5 represent high-emission conditions for the future. From an uncertainty standpoint, future scenarios are also not necessarily accurate representations of the future but rather plausible cases. Therefore, the numerical ranges represented should not be regarded as accurate, especially when bias correction may alter the signal produced in raw climate model output.

This previous discussion begs the question of the costs versus benefit to end users of employing a single dynamically downscaled dataset versus an ensemble of GCMs for extreme analysis. Given that the trends generally tended to agree among all datasets, with some exceptions in raw time series trends (Table 4), and since the dynamically downscaled datasets produced maximum values that were either within or only slightly exceeding that of GCMs, it is likely acceptable for users to rely on either dataset for understanding extremes. Depending on the application and resources available to users, results of this study suggest that relying on as many possible raw GCMs, downscaling methods and scenarios is still likely the best way of understanding uncertainty and developing robust local information on climate trends. Ensembles do offer advantages of being able to more specifically characterize the full distribution of plausible futures in an area, which is advantageous in both bottom-up and top-down analyses and planning.

Regardless of which datasets users rely on, it is critical that they regard the fact that any downscaled dataset is only a representation of historical or future conditions and that there is inherent uncertainty in the way models are conceptualized and scenarios run. Although dynamically downscaled datasets offer a more sophisticated conceptualization of the local climate, they are still driven by GCM boundary conditions and make additional assumptions in their parameterization, which need to be considered by users.

Please cite this article in press as: Razavi, T., et al., Climate Risk Management (2016), http://dx.doi.org/10.1016/j.crm.2016.06.002

Table 8
Estimates of temperature and precipitation extreme indices for various historical and future normal periods before and after bias correction.

Variable	Observed		CIMP5 ensemble (median)						CanRCM4						PRECIS mean		
	1960s	1990s	2020s		2050s		2080s		2020s		2050s		2080s		2020s	2050s	2080s
			rcp4.5	rcp8.5	rcp4.5	rcp8.5	rcp4.5	rcp8.5	rcp4.5	rcp8.5	rcp4.5	rcp8.5	rcp4.5	rcp8.5	A2		
Before bias-correction																	
TXx(°C)	36.5	37.1	39.73	39.9	41	43	40.6	45.2	47.3	46.9	49.2	50.4	49	51	47	49	52
TXn(°C)	−18	−17	−16	−16	−14	−12	−12.7	−8.1	−13.7	−8.5	−10	−7	−11	–	−13	−9	−8
TNx(°C)	23	25	28	28	28	29	28	31	30.8	30	30	30	32	32	32	35	38
TNn(°C)	−27	−27	−27	−27	−25	−21	−22	−15	−26	−26	−20	−20	−25	−25	−21	−16	−15
FD(days/year)	141	131	116	115	109	101	104	83	83	88	62	66	57	57	111	93	76
ID(days/year)	58	51	47	49	49	44	49	30	18	10	8	4	7	3	30	17	8
SU(days/year)	62	63	72	72	82	90	89	109	135	135	139	145	147	163	91	106	125
TR(days/year)	4	7	36	38	49	60	58	85	36	35	47	45	56	54	40	62	78
RX1day(mm)	60	66	55	56	60	62	57	64	146	138	164	226	126	138	175	170	162
RX5day(mm)	98	87	105	102	113	115	108	121	152	164	208	246	186	164	266	216	238
SDII(mm)	6.5	6.3	5.8	5.8	6	6.1	6.1	6.4	7.7	8.1	7.9	8	8	8.1	8	9	9
R10mm(days/year)	26	26	26	26	28	28	29	30	27	27	27	27	25	27	26	26	28
R20mm(days/year)	6	6	7	7	8	8	8	9	9	12	11	11	10	12	10	11	12
CDD(days)	31	25	22	24	24	26	25	26	43	53	24	24	39	53	37	37	37
CWD(days)	10	10	18	17	17	18	18	18	10	16	8	12	16	16	8	12	8
R95p(mm/year)	141	142	239	247	277	283	280	327	212	278	242	271	269	278	288	319	349
R99p(mm/year)	55	54	71	77	91	104	103	149	81	106	86	99	107.2	106	108	124	130
PRCPTOT(mm/year)	848	873	1001	1002	1006	996	1026	1024	916	992	952	985	922	992	878	900	936
After bias-correction																	
TXx(°C)	36.5	37.1	38.8	39.5	40.2	42.5	40.9	44.8	38.1	38.9	39.7	40.7	39.8	41.7	41.7	43.1	45.2
TXn(°C)	−18.9	−17.9	−16.2	−17	−13.9	−13.1	−12.3	−9	−17.8	−13.2	−14.2	−10.7	−10.7	−8.8	−14.4	−10.2	−8.7
TNx(°C)	23.6	25.1	26.7	26.8	27	29	27.9	31.7	26.1	26	25.9	26	26	27.3	28.9	31	33
TNn(°C)	−27.5	−27	−25.5	−25.3	−23.5	−22.8	−21.3	−17.9	−25.9	−24.7	−21.3	−23.4	−23.5	−24.4	−24	−18.8	−17.3
FD(days/year)	141	131	122	120	111	101	104	76	126	130	107	111	112	102	119	102	86
ID(days/year)	58	51	43	41	34	28	31	17	45	38	31	22	23	10	37	23	13
SU(days/year)	62	63	84	84	97	106	107	129	88	81	93	101	102	128	83	99	124
TR(days/year)	4	7	13	15	20	30	27	55	12	12	19	18	18	23	15	32	46
RX1day(mm)	60	66	80	81	72	88	75	85	94	130	140	158	114	131	144	163	117
RX5day(mm)	98	87	119	127	126	135	129	145	124	172	180	180	170	143	227	200	156
SDII(mm)	6.5	6.3	6.5	6.8	6.7	7	6.8	7.4	6.7	6.6	6.7	6.8	6.7	6.9	6.6	6.9	7.1
R10mm(days/year)	26	26	26	27	28	29	28	30	25	23	26	26	23	25	23	24	26
R20mm(days/year)	6	6	7	8	8	10	8	11	7	7	8	8	7	9	6	8	8
CDD(days)	31	25	26	25	25	29	27	27	24	24	21	24	28	21	26	30	25
CWD(days)	10	10	12	11	12	12	12	12	10	10	11	13	16	12	9	12	9
R95p(mm/year)	141	142	192	187	214	234	224	281	203	199	221	248	228	271	253	297	307
R99p(mm/year)	55	54	59	71	83	91	92	119	74	81	82	86	93	98	112	125	139
PRCPTOT(mm/year)	848	873	881	896	913	946	927	991	899	892	925	940	891	965	871	878	888

Table 9
Observed climate extreme indices in 1960s and 1990s and uncertainty bound of 10th and 90th percentile of bias−corrected and non-bias-corrected climate indices in 2020s, 2050s, and 2080s.

Variable	Observed		Uncertainty bound of climate model projections					
	1960s	1990s	2020s		2050s		2080s	
			10th P	90th P	10th P	90th P	10th P	90th P
TXx(°C)	36.5	37.1	39.1	45.6	40.8	47.8	41.1	48.1
TXn(°C)	−18.9	−17.9	−16.6	−13.7	−13.7	−10.1	−11.6	−8.6
TNx(°C)	23.6	25.1	26.7	30.3	27.3	30.3	28.1	32.6
TNn(°C)	−27.5	−27.0	−26.0	−24.9	−23.3	−20.1	−24.2	−17.5
FD(days/year)	141	131	112	122	95	109	76	104
ID(days/year)	58	51	32	45	18	33	9	28
SU(days/year)	62	63	82	91	94	106	108	129
TR(days/year)	4	7	14	36	23	49	32	58
RX1day(mm)	60.9	66.0	80.5	142.8	76.3	164.3	77.8	130.5
RX5day(mm)	98.6	87.3	121.1	170.5	128.7	206.4	132.8	168.9
SDII(mm)	6.5	6.3	6.5	7.5	6.7	7.7	6.7	7.9
R10mm(days/year)	26	26	25	27	26	28	25	29
R20mm(days/year)	6	6	7	9	8	11	8	11
CDD(days)	31	25	24	34	24	28	25	35
CWD(days)	10	10	10	15	12	13	12	16
R95p(mm/year)	141.0	142.7	200.8	252.2	236.3	282.0	269.7	301.3
R99p(mm/year)	55.9	54.7	72.5	100.3	86.6	103.6	99.8	128.1
PRCPTOT(mm/year)	848	873	884	973	916	977	923	992

5. Conclusions

This study focussed on analyzing past and future trends in local extreme climate (temperature and precipitation) in Hamilton region in Ontario, Canada, using a range of downscaled climate model outputs. Data analysis also included bias-correction to elucidate how this commonly applied transformation affects finding and interpretation of trends in extreme indices.

Results of this study demonstrated that statistical bias-correction can significantly reduce the RMSE of most of the annual extreme indices of temperature. For the precipitation extreme indices bias correction did not improve the representation of annual extreme indices. Bias-corrected and non-bias corrected indices indicated similar increasing and decreasing trends for most of the indices, however there was still great variability in the range of values among datasets. No single dataset was consistently more accurate than any other over the historical period. All climate models predicted an increasing trend for total wet day precipitation (PRCPTOT) and maximum consecutive wet days (CWD), very heavy precipitation days (R20mm), Summer Days (SU) and Tropical Nights (TR) and a decreasing trend for Frost Days (FD) and Ice Days (ID) in 2020s, 2050s, and 2080s compared to present.

With respect to comparing different climate model datasets, it was evident that over the historical period, the CMIP5 dataset consistently set the largest range of values. The CanRCM4 dataset projected future values in the upper range of the CMIP5 ensemble, while the PRECIS dataset's values were consistently lower. Ultimately, this suggests that from a usage standpoint, no single dataset can be regarded as "better" than any other. That being said, there are distinct advantages to previously recommended guidance in the climate modeling community of users relying on an ensemble of climate model datasets whether using a top-down or bottom-up approach to assessing and responding to climate extremes.

Acknowledgments

We acknowledge help and support from all individuals and organizations for this work. In particular thanks to funding agencies including Mitcas, City of Hamilton, Hamilton Conservation Authority (HCA), Matrix Solution Inc. Part of this work was funded by the National Science and Engineering Research Council (NSERC) through the NSERC Canadian Flood-Net Kind support and data from the Ontario Climate Consortium (OCC), McMaster Centre for Climate Change (MCCC), Ministry of Environment and Climate Change (MOECC) and Environment Canada (EC) are also acknowledged. We also acknowledge the World Climate Research Programme's Working Group on Coupled Modelling, which is responsible for CMIP, and we thank the climate modeling groups (listed in Table A) for producing and making available their model output.

Appendix A
List of CIMP5 models and their ensemble datasets.

Modeling center (or Group)	Institute ID	Model name
Commonwealth Scientific and Industrial Research Organization (CSIRO) and Bureau of Meteorology (BOM), Australia	CSIRO – BOM	ACCESS 1.0, ACCESS 1.3
Beijing Climate Center, China Meteorological Administration	BCC	BCC-CSM1.1, BCC-CSM1.1(m)
Instituto Nacional de Pesquisas Espaciais (National Institute for Space Research)	INPE	BESM OA 2.3*
College of Global Change and Earth System Science, Beijing Normal University	GCESS	BNU-ESM
Canadian Center for Climate Modelling and Analysis	CCCMA	CanESM2, CanCM4, CanAM4
University of Miami – RSMAS	RSMAS	CCSM4 (RSMAS)*
National Center for Atmospheric Research	NCAR	CCSM4
Community Earth System Model Contributors	NSF-DOE-NCAR	CESM1(BGC), CESM1(CAM5), CESM1(CAM5.1, FV2), CESM1(FASTCHEM), CESM1(WACCM)
Center for Ocean-Land-Atmosphere Studies and National Centers for Environmental Prediction	COLA and NCEP	CFSv2-2011
Centro Euro-Mediterraneo per | Cambiamenti Climatici	CMCC	CMCC-CESM, CMCC-CM, CMCC-CMS
Centre National de Recherches Mètéorologiques/Centre Européen de Recherche et Formation Avancée en Calcul Scientifique	CNRM – CERFACS	CNRM – CM5 CNRM – CM5-2
Commonwealth Scientific and Industrial Research Organization in collaboration with Queensland Climate Change center of Excellence	CSIRO-QCCE	CSIRO-MK3.6.0
EC-EARTH consortium	EC-EARTH	EC-EARTH
LASG, Institute of Atmospheric Physics, Chinese Academy of Sciences and CESS, Tsinghua University	LASG-CESS	FGOALS-g2
LASG, Institute of Atmospheric Physics, Chinese Academy of Sciences	LASG-IAP	FGOALS-g1, FGOALS-s2
The First Institute of Oceanography, SOA, China	FIO	FIO-ESM
NASA Global Modeling and Assimilation Office	NASA GMAO	GEOS-5
NOAA Geophysical Fluid Dynamics Laboratory	NOAA GFDL	GFDL-CM2.1, GFDL-CM3, GFDL-ESM2G, GFDL-ESM2M, GFDL-HIRAM-C180, GFDL-HIRAM-C360
NASA Goddard Institute for Space Studies	NASA GISS	GISS-E2-H, GISS-E2-H-CC, GISS-E2-R, GISS-E2-R-CC
National Institute of Meteorological Research/Korea Meteorological Administration	NIMR/KMA	HadGEM2-AO
Met Office Hadley Centre (additional HadGEM2-ES realizations contributed by Instituto Nacional de Pesquisas Espaciais)	MOHC (additional realizations by INPE)	HadCM3, HadGEM2-CC, HadGEM2-ES, HadGEM2-A
Institute for Numerical Mathematics	INM	INM-CM4
Institut Pierre-Simon Laplace	IPSL	IPSL-CM5A-LR, IPSL-CM5A-MR, IPSL-CM5B-LR
Japan Agency for Marine-Earth Sciences and Technology, Atmosphere and Ocean Research Institute (The University of Tokyo) and National Institute for Environmental Studies	MIROC	MIROC-ESM, MIROC-ESM-CHEM
Atmosphere and Ocean Research Institute (The University of Tokyo), and National Institute for Environmental Studies, and Japan Agency for Marine-Earth Science and Technology	MIROC	MIROC-ESM, MIROC-ESM-CHEM
Max-Planck-Institut for Meteorologie (Max Planck Institute for Meteorology)	MPI-M	MPI-ESM-MR, MPI-ESM-LR, MPI-ESM-P
Meteorological Research Institute	MRI	MRI-AGCM3.2H, MRI-AGCM3.2S, MRI-CGCM3, MRI-ESM1
Nonhydrostatic Icosahedra Atmospheric Model Group	NICAM	NICAM.09
Norwegian Climate Centre	NCC	NorESM1-M, NorESM1-ME

References

Baró, F., Chaparro, L., Gómez-Baggethun, E., Langemeyer, J., Nowak, D.J., Terradas, J., 2014. Contribution of ecosystem services to air quality and climate change mitigation policies: the case of urban forests in Barcelona, Spain. Ambio 43, 466–479. http://dx.doi.org/10.1007/s13280-014-0507-x.
Bhave, A.G., Mishra, A., Raghuwanshi, N.S., 2014. A combined bottom-up and top-down approach for assessment of climate change adaptation options. J. Hydrol. 518, 150–161. http://dx.doi.org/10.1016/j.jhydrol.2013.08.039.
Brekke, L.D., Thrasher, B.L., Maurer, E.P., Pruitt, T., 2013. Downscaled CMIP3 and CMIP5 Climate and Hydrology Projections: Release of Downscaled CMIP5 Climate Projections, Comparison with preceding Information, and Summary of User Needs 116p.
Brown, C., Wilby, R.L.R.L., 2012. An alternate approach to assessing climate risks. Eos, Trans. Am. Geophys. Union 92, 92–94. http://dx.doi.org/10.1029/2012EO410001.
Brown, C., Ghile, Y., Laverty, M., Li, K., 2012. Decision scaling: linking bottom-up vulnerability analysis with climate projections in the water sector. Water Resour. Res. 48, 1–12. http://dx.doi.org/10.1029/2011WR011212.
Bürger, G., Murdock, T.Q., Werner, A.T., Sobie, S.R., Cannon, A.J., 2012. Downscaling extremes—an intercomparison of multiple statistical methods for present climate. J. Clim. 25, 4366–4388. http://dx.doi.org/10.1175/JCLI-D-11-00408.1.
Environment Canada, 2014. Historical Climate Data [WWW Document]. Gov, Canada.
Candau, J.-N., Fleming, R.A., 2011. Forecasting the response of spruce budworm defoliation to climate change in Ontario. Can. J. For. Res. 41, 1948–1960. http://dx.doi.org/10.1139/x11-134.
Charron, I., 2014. A Guidebook on Climate Scenarios: Using Climate Information to Guide Adaptation Research and Decisions.

Please cite this article in press as: Razavi, T., et al.. Climate Risk Management (2016), http://dx.doi.org/10.1016/j.crm.2016.06.002

Cheng, C.S., Auld, H., Li, Q., Li, G., 2012. Possible impacts of climate change on extreme weather events at local scale in south-central Canada. Clim. Change 112, 963–979. http://dx.doi.org/10.1007/s10584-011-0252-0.

Donat, M.G., Peterson, T.C., Brunet, M., King, A.D., Almazroui, M., Kolli, R.K., Boucherf, D., Al-Mulla, A.Y., Nour, A.Y., Aly, A.A., Nada, T.A.A., Semawi, M.M., Al Dashti, H.A., Salhab, T.G., El Fadli, K.I., Muftah, M.K., Dah Eida, S., Badi, W., Driouech, F., El Rhaz, K., Abubaker, M.J.Y., Ghulam, A.S., Erayah, A.S., Mansour, M. Ben, Alabdouli, W.O., Al Dhanhani, J.S., Al Shekaili, M.N., 2014. Changes in extreme temperature and precipitation in the Arab region: long-term trends and variability related to ENSO and NAO. Int. J. Climatol. 34, 581–592. http://dx.doi.org/10.1002/joc.3707.

dos Santos, C.A.C., Neale, C.M.U., Rao, T.V.R., da Silva, B.B., 2011. Trends in indices for extremes in daily temperature and precipitation over Utah, USA. Int. J. Climatol. 31, 1813–1822. http://dx.doi.org/10.1002/joc.2205.

EBNFLO Environmental, AquaResource Inc., 2010. Guide for Assessment of Hydrologic Effects of Climate Change in Ontario.

Ehret, U., Zehe, E., Wulfmeyer, V., Warrach-Sagi, K., Liebert, J., 2012. *HESS Opinions* "Should we apply bias correction to global and regional climate model data?". Hydrol. Earth Syst. Sci. 16, 3391–3404. http://dx.doi.org/10.5194/hess-16-3391-2012.

Engineers Canada, 2015. Public Infrastructure Engineering Vulnerabilty Committee (PIEVC) Engineering Protocol [WWW Document].

Field, C.B., Barros, V.R., Mach, K.J., Mastrandrea, M.D., van Aalst, M., Adger, W.N., Arent, D.J., Barnett, J., Betts, R., Bilir, T.E., Birkmann, J., Carmin, J., Chadee, D. D., Challinor, A.J., Chatterjee, M., Cramer, W., Davidson, D.J., Estrada, Y.O., Gattuso, J.-P., 2014. Technical summary. In: Climate Change 2014: Impacts, Adaptation, and Vulnerability. Part A: Global and Sectoral Aspects. Contribution of Working Group II to the Fifth Assessment Report of the Intergovernmental Panel on Climate Change. http://dx.doi.org/10.1016/j.renene.2009.11.012, Cambridge, UK. and New York, NY.

Honti, M., Scheidegger, A., Stamm, C., 2014. The importance of hydrological uncertainty assessment methods in climate change impact studies. Hydrol. Earth Syst. Sci. 18, 3301–3317. http://dx.doi.org/10.5194/hess-18-3301-2014.

ICLEI, 2010. Changing Climate, Changing Communities: Guide and Workbook for Municipal Climate Adaptation, Toronto ON.

Ines, A.V.M., Hansen, J.W., 2006. Bias correction of daily GCM rainfall for crop simulation studies. Agric. For. Meteorol. 138, 44–53. http://dx.doi.org/10.1016/j.agrformet.2006.03.009.

IPCC, 2012. Managing the Risks of Extreme Events and Disasters to Advance Climate Change Adaptation: A Special Report of Working Groups I and II of the Intergovernmental Panel on Climate Change. Cambridge University Press, Cambridge, UK. and New York, NY. http://dx.doi.org/10.1017/CBO9781139177245.

IPCC, 2014. Climate Change 2014: Impacts, Adaptation, and Vulnerability: Contribution to the Fifth Assessment Report of the Intergovernmental Panel on Climate Change. Cambridge University Press, Cambridge, UK. and New York, NY.

IPCC-TGICA, 2007. General guidelines on the use of scenario data for climate impact and adaptation assessment. Finnish Environ. Inst. 312, 66. http://dx.doi.org/10.1144/SP312.4.

Kang, Y., Khan, S., Ma, X., 2009. Climate change impacts on crop yield, crop water productivity and food security – a review. Prog. Nat. Sci. 19, 1665–1674. http://dx.doi.org/10.1016/j.pnsc.2009.08.001.

Kendall, M.G., 1955. Rank Correlation Methods. Griffin, London.

Mann, H.B., 1945. Nonparametric tests against trend. Econometrica 13, 245–259.

Matthews, S.N., Iverson, L.R., Peters, M.P., Prasad, A.M., Subburayalu, S., 2014. Assessing and comparing risk to climate changes among forested locations: implications for ecosystem services. Landscape Ecol. 29, 213–228. http://dx.doi.org/10.1007/s10980-013-9965-y.

Maurer, E.P., Brekke, L., Pruitt, T., Duffy, P.B., 2007. Fine-resolution climate projections enhance regional climate change impact studies. Eos. Trans. Am. Geophys. Union 88, 504. http://dx.doi.org/10.1029/2007EO470006.

McKenney, D.W., Hutchiinson, M.F., Papadopol, P., Lawrence, K., Pedlar, J., Campbell, K., Milewska, E., Hopkinson, R.F., Price, D., Owen, T., 2011. Customized spatial climate models for North America. Bull. Am. Meteorol. Soc. 92, 1611–1622. http://dx.doi.org/10.1175/2011BAMS3132.1.

Pasini, S., Torresan, S., Rizzi, J., Zabeo, A., Critto, A., Marcomini, A., 2012. Climate change impact assessment in Veneto and Friuli Plain groundwater. Part II: A spatially resolved regional risk assessment. Sci. Total Environ. 440, 219–235. http://dx.doi.org/10.1016/j.scitotenv.2012.06.096.

PNW Tribal Climate Change Project, 2013. A Tribal Planning Framework – Climate Change Adaptation Strategies by Sector.

Powell, E.J., Keim, B.D., 2015. Trends in daily temperature and precipitation extremes for the Southeastern United States: 1948–2012. J. Clim. 28, 1592–1612. http://dx.doi.org/10.1175/JCLI-D-14-00410.1.

Rogelj, J., Meinshausen, M., Knutti, R., 2012. Global warming under old and new scenarios using IPCC climate sensitivity range estimates. Nat. Clim. Change 2, 248–253.

Samuel, J., Coulibaly, P., Metcalfe, R.A., 2012. Evaluation of future flow variability in ungauged basins: validation of combined methods. Adv. Water Resour. 35, 121–140. http://dx.doi.org/10.1016/j.advwatres.2011.09.015.

Seidou, O., Ramsay, A., Nistor, I., 2012. Climate change impacts on extreme floods I: combining imperfect deterministic simulations and non-stationary frequency analysis. Nat. Hazards 61, 647–659. http://dx.doi.org/10.1007/s11069-011-0052-x.

Sharma, D., Gupta, A. Das, Babel, M.S., 2007. Spatial disaggregation of bias-corrected GCM precipitation for improved hydrologic simulation: Ping River Basin, Thailand. Hydrol. Earth Syst. Sci. Discuss. 11, 1373–1390. http://dx.doi.org/10.5194/hessd-4-35-2007.

Sillmann, J., Kharin, V.V., Zhang, X., Zwiers, F.W., Bronaugh, D., 2013. Climate extremes indices in the CMIP5 multimodel ensemble: Part 1. Model evaluation in the present climate. J. Geophys. Res. Atmos. 118, 1716–1733. http://dx.doi.org/10.1002/jgrd.50203.

Stocker, T.F., 2013. Climate Change 2013. The Physical Science Basis: Working Group I Contribution to the Fifth Assessment Report of the Intergovernmental Panel on Climate Change. Cambridge University Press, Chicago, USA.

Swanston, C., Janowiak, M., 2012. Forest Adaptation Resources: Climate Change Tools and Approaches for Land Managers 120.

Taylor, K.E., Stouffer, R.J., Meehl, G.A., 2012. An overview of CMIP5 and the experiment design. Bull. Am. Meteorol. Soc. 93, 485–498. http://dx.doi.org/10.1175/BAMS-D-11-00094.1.

Tebaldi, C., Knutti, R., 2007. The use of the multi-model ensemble in probabilistic climate projections. Philos. Trans. A. Math. Phys. Eng. Sci. 365, 2053–2075. http://dx.doi.org/10.1098/rsta.2007.2076.

Velázquez, J.A., Schmid, J., Ricard, S., Muerth, M.J., Gauvin St-Denis, B., Minville, M., Chaumont, D., Caya, D., Ludwig, R., Turcotte, R., 2012. An ensemble approach to assess hydrological models' contribution to uncertainties in the analysis of climate change impact on water resources. Hydrol. Earth Syst. Sci. Discuss. 9, 7441–7474. http://dx.doi.org/10.5194/hessd-9-7441-2012.

Wang, X., Gordon, H., 2013. Ontario Climate Change Data Portal. Available from: http://www.ontarioccdp.ca.

Wilby, R.L., Keenan, R., 2012. Adapting to flood risk under climate change. Prog. Phys. Geogr. 36, 348–378. http://dx.doi.org/10.1177/0309133312438908.

Wilby, R.L., Dawson, C.W., Murphy, C., O'Connor, P., Hawkins, E., 2014. The Statistical DownScaling Model – Decision Centric (SDSM-DC): conceptual basis and applications. Clim. Res. 61, 259–276. http://dx.doi.org/10.3354/cr01254.

Yao, Y., Luo, Y., Huang, J., Zhao, Z., 2013. Comparison of monthly temperature extremes simulated by CMIP3 and CMIP5 models. J. Clim. 26, 7692–7707. http://dx.doi.org/10.1175/JCLI-D-12-00560.1.

Zhang, X., Alexander, L., Hegerl, G.C., Jones, P., Tank, A.K., Peterson, T.C., Trewin, B., Zwiers, F.W., 2011. Indices for monitoring changes in extremes based on daily temperature and precipitation data. Wiley Interdiscip. Rev. Clim. Change 2, 851–870. http://dx.doi.org/10.1002/wcc.147.

Zhou, Y., Zwahlen, F., Wang, Y., Li, Y., 2010. Impact of climate change on irrigation requirements in terms of groundwater resources. Hydrogeol. J. 18, 1571–1582. http://dx.doi.org/10.1007/s10040-010-0627-8.